Chapter 10
Net Ecosystem Exchange of CO_2 in Permafrost Larch Ecosystems

Y. Nakai

10.1 Introduction

Carbon dioxide exchange between the ecosystem and the atmosphere would be a major component for carbon budget at boreal forests. In this chapter, net ecosystem exchange (NEE) of CO_2 at a permafrost larch ecosystem will be discussed, based on a micrometeorological (tower flux) measurement. Movement of CO_2 from ecosystem to atmosphere is customarily labeled as positive. The micrometeorological measurement can obtain NEE with a half-hourly time-resolution at an ecosystem scale. These temporal and spatial scales are advantages in carbon, water, and energy budget studies over ecological measurements.

Most studies of recent micrometeorological NEE measurements in boreal forest regions have been conducted in evergreen coniferous ecosystems and in broad-leaved mixed forests of aspen, birch, and other species (Jarvis et al. 2001); see, for example, the Boreal ecosystem–atmosphere study (BOREAS) in Canada (Sellers et al. 1997), the northern hemisphere climate-processes land-surface experiment (NOPEX) in Scandinavia (Halldin et al. 1999), and the EuroSiberian Carbonflux (Schulze et al. 1999) and the TCOS-Siberia (e.g., Shibistova et al. 2002; Röser et al. 2002) projects in Siberia.

On the other hand, deciduous conifer, i.e., larch, has only a few series of continuous micrometeorological measurements of NEE taken in northern Eurasia such as Russia (Dolman et al. 2004; Machimura et al. 2005; Nakai et al. 2005), Mongolia (Li et al. 2005), China (Wang et al. 2005), and Japan (Hirano et al. 2003; Wang et al. 2004), in spite of its growing locations distributed over extended areas. In these studies, the measurements conducted over the continuous permafrost are very limited. One could easily imagine reasons why so few studies carry out continuous measurements in the permafrost larch ecosystems. They are in regions of extremely cold and continental climate, and at geographically remote locations. Consequently, micrometeorological NEE data from permafrost larch forests of Siberia are expected to be highly valuable to the studies of global carbon budget.

Some pioneering micrometeorological measurements at a few *Larix gmelinii* forests in Yakutia in Northeastern Siberia were reported in the literatures. The ecosystem exchange of water vapor (Kelliher et al. 1997) and carbon dioxide (Hollinger

A. Osawa et al. (eds.), *Permafrost Ecosystems: Siberian Larch Forests*,
Ecological studies, Vol. 209, DOI 10.1007/978-1-4020-9693-8_10,

et al. 1995, 1998) was assessed at a stand located at south of Yakutsk during midsummer. The GAME Siberia, CREST/WECNoF (Ohta 2005), and TCOS-Siberia projects had long-term measurements in a larch forest at Spasskaya Pad Experimental Site near Yakutsk in the continuous permafrost area. At this site, Ohta et al. (2001) reported year-round measurements of heat and water vapor fluxes. Also Ohta et al. (2008) measured the inter-annual variation of water balance (see also Chap. 13, this Vol.). Dolman et al. (2004) estimated seasonal variation in NEE. Machimura et al. (2005) estimated NEE of 80–130 gC m^{-2} for seasons from May to September by a micrometeorological measurement at Neleger near Yakutsk. However, the average tree size at these stands near Yakutsk was larger (e.g., heights >10 m) than the size typical of larch forests on Siberian permafrost. Generally, average tree heights in the canopy layer of old *L. gmelinii* stands do not exceed 10 m in the continuous permafrost regions of Central Siberia (Abaimov et al. 1998; Bondarev 1997; Kajimoto et al. 1999; see also Chap. 7, this Vol.).

As described above, recent information on NEE of larch forests in Siberia is still limited to stands with relatively large individuals near Yakutsk. To gain better understanding of NEE for typical permafrost larch ecosystems, there should be more sites for tower flux measurement in permafrost region of Siberian taiga. As one of such sites, a tower flux measurement was initiated in 2004 to observe energy, water, and CO_2 above a mature larch stand near Tura, Central Siberia (Nakai et al. 2004). This site may warrant a long-term study since it has stand structure typical of old *L. gmelinii* forests of the region and was established on a plateau. Recently, enough metainformation was also obtained by intensive and extensive ecological studies at sites near the flux tower (Zyryanova and Shitova 1999; Zyryanova et al. 2000; Kajimoto et al. 1999, 2003; Abaimov et al. 2000; Osawa et al. 2000, 2003, 2004; Matsuura and Abaimov 2000; Tokuchi et al. 2004; Matsuura et al. 2005; see also related chapters, this Vol.).

The objectives of this study were to estimate seasonal and annual carbon dioxide exchange and to evaluate whether the gmelin larch (*Larix gmelinii*) ecosystem functions as a carbon sink or source. For those purposes, measurement should be continued for many years. Measured data may be useful for understanding function of permafrost larch ecosystems. In this chapter, half-hourly, daily, and seasonal changes in NEE of a permafrost larch ecosystem are shown, based on the flux measurements at Tura in 2004 (Nakai et al. 2008).

10.2 Study Site for Micrometeorological Measurements

In 2002, a 105-year-old stand of larch (*Larix gmelinii*) forest (Carbon Flux Site in Fig. 1.3, this Vol.), east of the village of Tura, was selected for micrometeorological measurements. A 20-m high wooden tower was constructed in 2003 within the settlement of Tura, and this prefabricated structure was transported to the study site by a helicopter (Fig.10.1) in August 2003. The equipment was set up and flux measurements started in early June 2004 (Fig. 10.2).

Fig. 10.1 A helicopter transporting the wooden tower to the study site. The tower was landing on the ground (Photo: Y. Matsuura)

Fig. 10.2 The tower equipped with all devices (Photo: Y. Nakai) *(see* Color Plates)

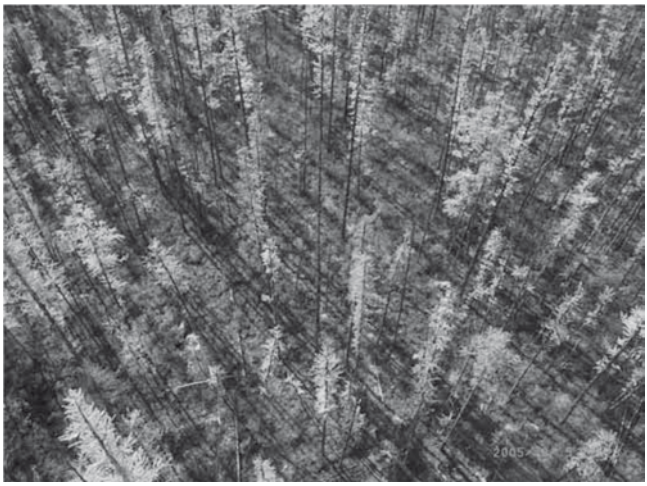

Fig. 10.3 Slender canopy of the larch trees in 105-year-old larch stand (Photo: Y. Nakai)

The site is on a slightly sloping terrace of the Nyzhnyaya Tunguska River with a northern aspect. It consists of a nearly even-aged stand of 105-year-old larch trees that originated from an intensive forest fire in late 1890s. The prevailing winds are westerly (Nakai et al. 2005). According to tree census data from four permanent plots near the flux tower (Kajimoto et al. 2004, 2007; see Table 6.1, this Vol.), stem density of living larch trees is about 5,480 trees ha^{-1}. Average diameter of the trees at breast height is 3.2 cm; mean tree height is 3.4 m. Individual tree crowns are slender and rarely overlap with one another (Fig. 10.3). Consequently, the stand has a very sparse canopy. Leaf biomass of the stand is 0.44 Mg ha^{-1}, and leaf area index (LAI; calculated as projected needle area) is ca. 0.6 ha ha^{-1} (details see Table 6.2, this Vol.). The leaves of the larch trees are nearly exclusively short shoot leaves and are often distributed throughout the length of the stem.

Soil type is cryosol with permafrost table existing within the upper one meter of the soil profile (Matsuura et al. 2005). The parent material is old fluvial deposit of the Nyzhnyaya Tungusuka River. Soil texture of the surface-active layer is clay rich. Ground surface is densely covered with lichen and moss as is seen commonly at high latitude boreal forests. This cover forms a thick porous layer of 10–30 cm in depth above the mineral soil, which functions as a heat insulator above the mineral soil. Climate data of Tura from a station with long-term observations (Lydolph 1977) are shown in Fig.10.4. According to the statistics of 1968–1995 observations at the station, annual mean air temperature is –9°C and annual total precipitation is 360 mm. About 45% of the annual precipitation falls between June and August. More detailed climatic information will be described in the next section.

Carbon dioxide, water vapor, heat, and momentum fluxes were measured at the top of the 20-m tall tower from June to early September, using the eddy covariance technique. Here, momentum flux can be calculated as covariance between horizontal

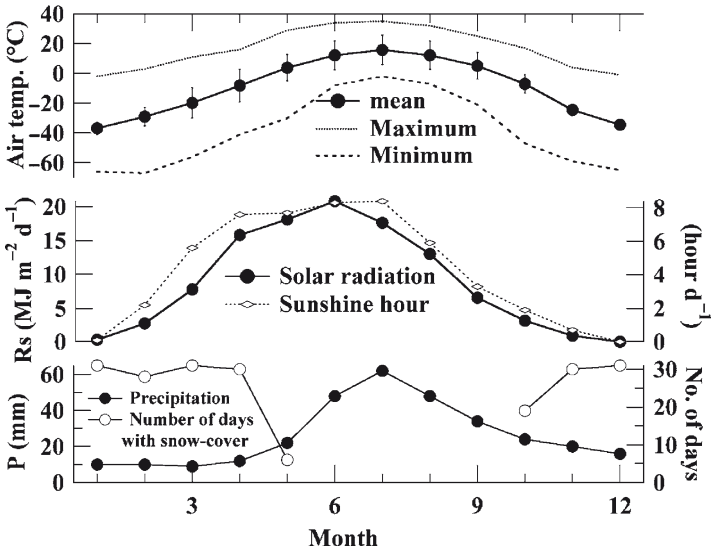

Fig. 10.4 Monthly climate variation of Tura. Error bar with monthly mean air temperature indicates mean daily difference. Data from Lydolph (1977)

wind and vertical wind. A three-dimensional sonic anemo-thermometer and a fast-response open-path infrared CO_2/H_2O gas analyzer (IRGA) were set at the top of the tower (see Table 10.1 for measurement sensors). Voltage signals from these eddy sensors were recorded at 10 Hz with a data logger (CR-5000, Campbell). The correction for angle of attack errors (Nakai et al. 2006) was applied to raw sonic wind data. Quality-control procedures designed by FFPRI FluxNet (Ohtani et al. 2005) were applied to the raw data as follows. First, graphs of the raw eddy time-series data plotted for an interval of every 30-min were visually checked. The noise-bearing data due to wetting on the sensor surfaces were excluded from further flux calculations. Second, within each half-hour observation, spikes and abnormal values out of plausible physical ranges, absolute variance, discontinuity, and stationarity were checked, using the procedures of Vickers and Mahrt (1997) and Foken and Wichura (1996). Coordinate axes for the wind field were rotated twice, so that the mean lateral and vertical velocities were zero (McMillen 1988). Humidity correction to sonic temperature and linear trends removal in scalar components (sonic temperature, water vapor, and CO_2 mixing ratio) were conducted. Water vapor and CO_2 fluxes were corrected for the air density effects using heat and water vapor fluctuation (WPL correction proposed by Webb et al. 1980). After the flux calculations, half-hourly fluxes with absolute angles of principal wind flow against a horizon >10°, measurable precipitation, or friction velocity <0.2 $m\,s^{-1}$ were excluded.

NEE between forest and the atmosphere can be computed as the sum of eddy covariance flux and storage change in CO_2 below the eddy flux measurement height (20 m in this case). The method by Hollinger et al. (1994) was employed for

Table 10.1 List of measurement items, heights, sensors for the micrometeorological observation

Measurement item	Height (m)	Sensor		
		Type	Model No.	Company
Fast response 3D-wind and sonic temperature	20 m = top of the tower	Sonic anemometer	R3	Gill
CO_2 and water vapor density		Open-path infrared gas analyzer	Li-7500	LiCor
Air temperature		Resistive platinum thermometer	HMP-45D	Vaisala
Relative humidity		Capacitive humidity sensor		
Wind speed and direction		Propeller anemometer	5103	R.M. Young
Rainfall		Tipping bucket rain gauge	T34	Ohta Keiki
Air pressure	18 m	Capacitive pressure sensor	PTB210	Vaisala
Shortwave – and Longwave radiation	20 m, down- & upward-	Radiation sensor	CNR1	Kip&Zonnen
Photosynthetic active radiation		Quantum sensor	Li-190SB	LiCor
Shortwave radiation at floor	1.1 m	Radiation sensor	CM03	Kip&Zonen
Photosynthetic active radiation at floor		Quantum sensor	Li-190SB	LiCor
Soil temperature	0.05, 0.1, 0.2, 0.4, 0.5 m	Resistive platinum thermometer	JIS-Pt100 4-wire	
Soil moisture		TDR sensor	CS616	Campbell
Soil heat flux	0.02, 0.05 m (depth)	Heat flux plate	HF-01	REBS

estimating the storage term since profile of CO_2 concentration was not measured at the site. However, the storage change in CO_2 should be verified by comparing it with profile measurements, because the estimates of storage changes here are uncertain, especially in half-hourly resolution.

Energy balance closure was examined to evaluate the surface flux measurements. The sum of turbulent energy fluxes is frequently less by 20% or more than the available radiative energy in many field measurements (e.g., Wilson et al. 2002). In this study, energy closure for quality-assured dataset was expressed by linear regressions as shown in Fig.10.5, where H is sensible heat flux, LE is latent heat flux, Rn is net radiation, and G is ground heat flux. *Left hand side* of Fig.10.5 (half-hourly time-resolution) revealed imbalance of total turbulent energy flux (H+LE) to some 40% of total radiative energy flux (Rn-G). On the other hand, right hand side of Fig.10.5 (daily time-resolution) shows much better agreement of total turbulent energy flux and total radiative energy flux. Such imbalance in half-hourly data might be due to the storage terms in sensible and latent heat fluxes, and to ignoring the latent heat of ice melting in the soil. Careful and detailed analysis of energy fluxes would still be needed for further discussion of energy balance closure.

Micrometeorological variables were also measured at the top of the tower: air temperature, relative humidity, wind speed and direction, precipitation, air pressure, shortwave, long-wave, and photosynthetic active radiation for both downward- and upward-direction. Soil temperature, moisture, and soil heat flux had been measured since late July 2004 (see Table 10.1 for measurement sensors with height or depth). For all micrometeorological variables, a half-hourly average was calculated and recorded with a data-logger (CR-10X, Campbell). Electricity for all devices was supplied with six solar panels (110 W maximum for each) through deep cycle batteries. A whole integrated measurement system (CFX-N1, Climatec, Inc.) had been operating steadily.

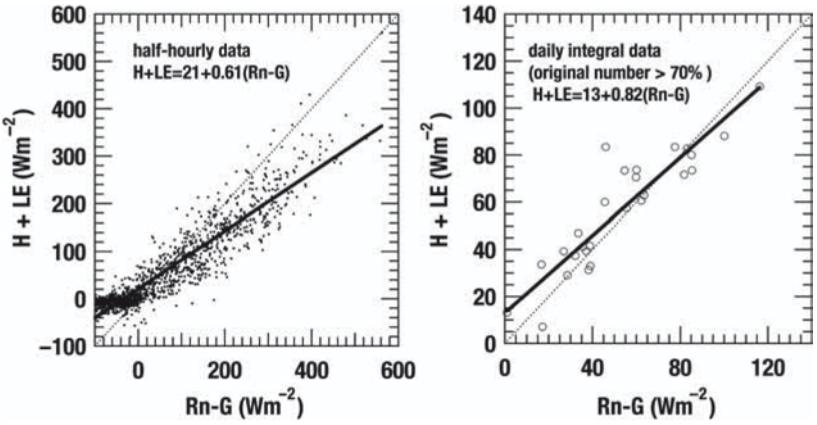

Fig. 10.5 Energy balance closure for observed energy fluxes. *H* sensible heat flux; *LE* latent heat flux; *Rn* net radiation; *G* ground heat flux; Total turbulent energy fluxes (H+LE) are plotted against total radiative energy fluxes (Rn-G)

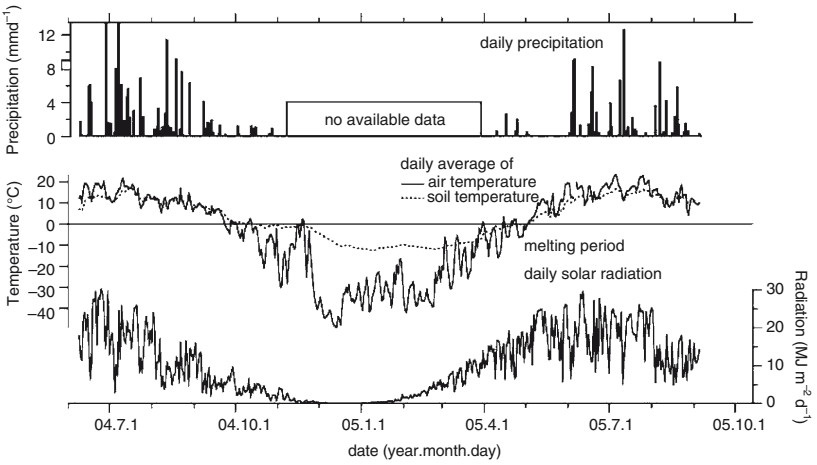

Fig. 10.6 Principal meteorological variations at Tura station of Russian Federal Service of Hydro-Meteorology from June 2004 to September 2005 (located in the residential area of Tura; see Fig. 1.3, this Vol.)

At Tura station of the Russian Federal Service of Hydro-Meteorology (located in a residential area of Tura; see Fig. 1.3, this Vol.), a year-round measurement was initiated for standard meteorological variables such as air temperature, humidity, solar radiation, wind speed, and precipitation. This provided additional meteorological data (Fig. 10.6) to those from the tower flux measurements. The year-round meteorological data help estimation of fluxes in early spring and late autumn when access to the tower site was difficult owing to instability of river ice, and provided basic data for annual NEE estimation (Nakai et al. 2007).

10.3 Meteorological Condition and Features of the Measurement Site

Monthly mean air temperature and total precipitation in the summer months (June, July, August) at the study site in 2004 are compared with the 30-year averages (1960–1989) recorded at the station of Russian Federal Service of Hydro-Meteorology in Tura (Table 10.2): monthly solar radiation in the summer 2004 is compared with climatic average values from Lydolph (1977). Mean monthly air temperature for 2004 was higher in June, but lower in July and August. Monthly precipitation was approximately half in June, but about the same in July and August. The temperature of the mineral soil surface under the lichen- or moss-litter layer, being affected by the permafrost, was nearly 0°C in June, and showed a maximum in July, decreasing in August, but was higher than that in June.

Daily climate variables are shown in Fig. 10.7. More than three quarters of the days in June were sunny (Fig. 10.7a). There were only several days of occasional showers.

Table 10.2 Meteorological characteristics of summer months at Tura, compared to long-term climatic mean values

	Year	June	July	August
Mean Air temperature (°C)	1960–89	12.4	16.9	13.1
	2004	16.0	14.5	10.8
Total Precipitation (mm)	1960–89	52	59	54
	2004	34	61	50
Total Solar radiation (MJ m^{-2})	[a]	624	546	390
	2004	624	524	326
Mean temperature at Mineral Soil surface (°C)	2004	1.5	4.8	3.1
Number of Day with precipitation >0 (mm d^{-1})	2004	9	18	16
Number of Days with maximum VPD[b] >1.5 kPa	2004	19	12	3

[a]Data from Lydolph (1977)
[b]Vapor pressure deficit

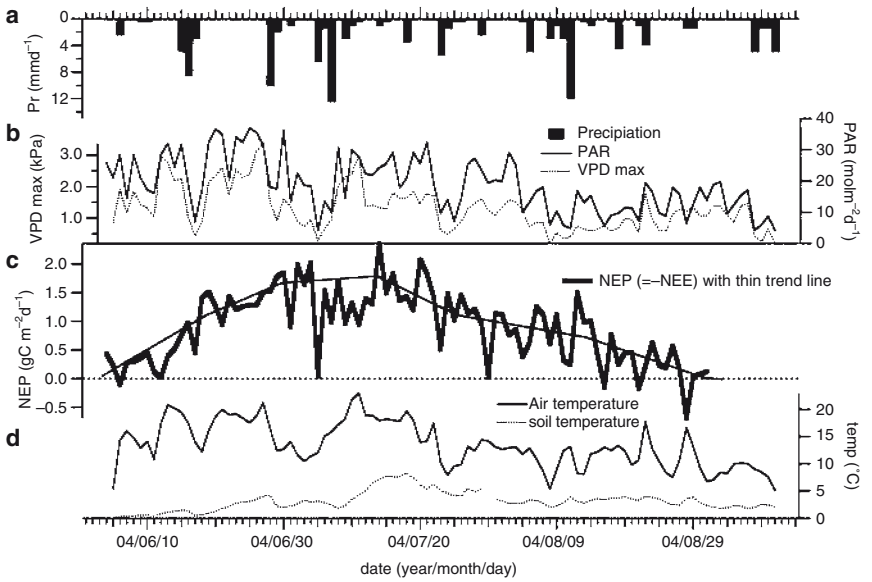

Fig. 10.7 Daily time-series of (**a**) precipitation (Pr), (**b**) daily maximum of vapor pressure deficit (VPDmax), photosynthetic active radiation (PAR), (**c**) net ecosystem production (NEP = −NEE), and (**d**) air temperature, and soil temperature (at 0.05 m depth of the mineral soil layer)

In both July and August, a majority of the days had rain, which was weaker and longer than in June. Total precipitation during the whole period was 125.5 mm (41 days with rainfall). In August, daily photosynthetic active radiation (PAR in Fig.10.7b) was considerably less than that in June and July, as the long-term average of monthly total

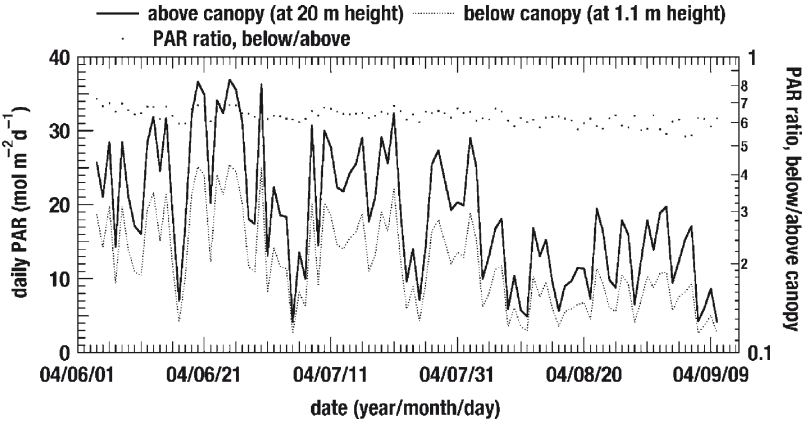

Fig. 10.8 Variation in daily photosynthetic active radiation (PAR) above (at 20 m height above ground) and below (at 1.1 m above the ground) the larch canopy

solar radiation reveals (Table 10.2). Average air temperature was 13.5°C throughout the measurement period (Fig. 10.7d). Daily maximum of vapor pressure deficit (VPDmax in Fig.10.7b) was generally higher in June and early July than in the later period.

Variations of the daily sums of photosynthetic active radiation (PAR) above the canopy (at 20 m height) and at the ground during the growing season are shown in Fig. 10.8. Day-to-day variations in PAR are large enough to obscure the seasonal change, though monthly PAR was the highest in June and lowest in August among the three months in summer. PAR at the ground was reduced to 55–70% of the global PAR above the canopy, as shown by PAR ratio (see dots in Fig. 10.8). This indicates that light interception by the larch canopy is not likely to limit the growth of ground vegetation. Dense ground vegetation under a sparse larch canopy in the permafrost forests might play a significant role in NEE, though seasonal variation in NEE during early growing season appears synchronized with larch needle development (for details see Sect. 10.4). Partitioning of CO_2 exchange into tree canopy and ground vegetation should be carried out to understand ecosystem function and its relationship to ecosystem structure.

10.4 Intensity and Seasonal Variations in Net Ecosystem Exchange and Larch Tree Phenology

Average diurnal cycles of NEE, PAR, and air temperature are indicated for each of 10-day periods in Fig. 10.9. Slightly negative NEE values of −1 μmol $m^{-2} s^{-1}$ at its minimum were observed during the daytime in early June. This indicates very weak net CO_2 uptake, though the open-path Infrared gas analyzer has a problem of

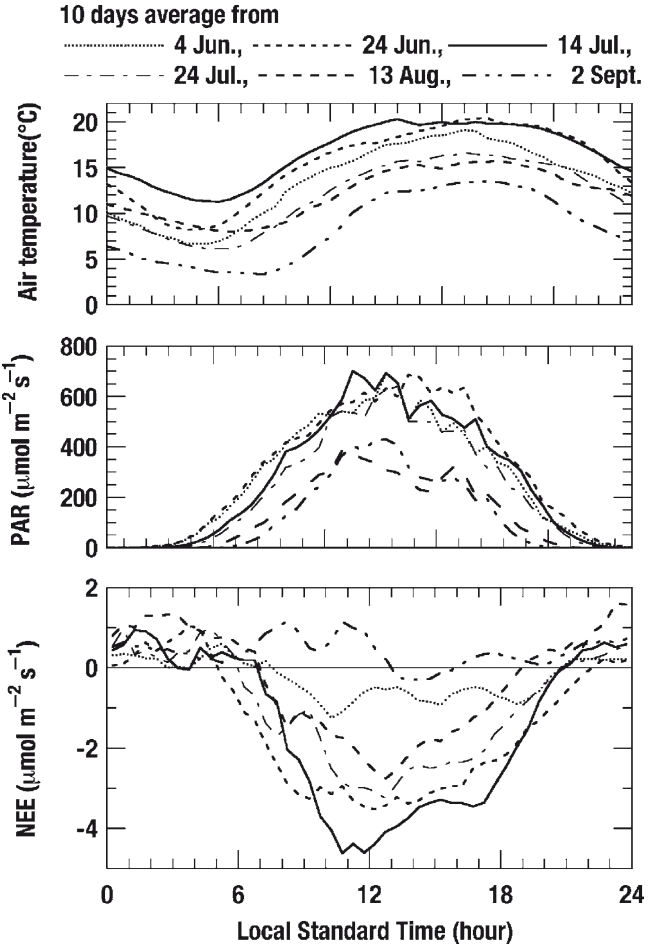

Fig. 10.9 Average diurnal cycles of NEE, PAR, and air temperature. Each line represents the average for 10-day periods: (a) 4–13 June; (b) 24 June–3 July; (c) 14–23 July; (d) 24 July–2 August; (e) 13–22 August; and (f) 2–11 September

underestimating NEE under a cold condition (e.g., Grelle and Burba 2007). In the beginning of June, soil surface started to melt and buds of larch trees had already broken. Larch needles did not flush for a few days after the bud break when air temperature was under 10°C, after which the needle flush began and was almost completed by the middle of June.

Daytime minimum of NEE reached −4 μmol $m^{-2} s^{-1}$ in late June (see lower graph in Fig.10.9). Furthermore, daytime minimum NEE of −5 μmol $m^{-2} s^{-1}$ was observed in mid July when NEE was at its lowest of the year and photosynthesis was likely to be most active. In late July, daytime minimum NEE became −3 μmol $m^{-2} s^{-1}$, which is equal to or larger than that in late June. In mid-August, NEE was little larger than

in late July, but still negative. The NEE was mostly in the positive range even during the daytime in early September when the leaves began to change color.

During four 10-day periods (10 days beginning on June 4, June 24, July14, and July 24), photosynthetic active radiation (PAR) showed similar values with each other (see middle graph in Fig. 10.9) – air temperature was probably high enough for photosynthesis (see upper graph in Fig. 10.9). However, NEE was clearly different with each other among these periods. Biological factors such as increased photosynthetic ability and CO_2 uptake of larch needles must promote Net Ecosystem Production (NEP = −NEE) from early June to early July, but the decrease in radiation and air temperature from mid-August to September should reduce the net uptake.

Later, based on daily integral of Net Ecosystem Production (NEP = −NEE), seasonal variation in NEE from the viewpoint of biological factors (such as photosynthetic ability) and environmental factors (such as air temperature and PAR) will be described again.

The relationship between NEE and absorbed PAR is approximated using a Michaelis-Menten type rectangular hyperbola (Ruimy et al. 1995):

$$\mathrm{NEE} = -P\max \cdot \frac{\mathrm{APAR}}{\mathrm{APAR} + \dfrac{P\max}{\alpha}} + Reco \tag{10.1}$$

where Pmax is maximum photosynthetic rate, α is initial light-use efficiency of the ecosystem, and Reco is ecosystem respiration. For light intensity of the ecosystem, absorbed photosynthetic active radiation (APAR) was used here, which was derived as incident PAR above the forest canopy minus reflective PAR. The relationship between daytime NEE and APAR was examined for every 10-day period, then it was approximated by applying Eq. (10.1). As shown in Fig.10.10, CO_2 uptake of the ecosystem was significantly lower in early June and early September than in other periods. Saturation of the CO_2 uptake against light intensity occurred approximately at APAR >500 μmol m^{-2} s^{-1} between mid-June and mid-August.

To estimate daily and seasonally integrated NEE, missing data of half-hourly NEE were filled with values (the so-called "gap-filling"). Here, gaps mean missing data due to device troubles or rejection by data quality control. The gaps that consisted of one or two points were filled with linear interpolation using data at both sides of each gap. For longer gaps during the daytime, regression models of Eq. (10.1) were used. Also, the longer gaps during nighttime were filled with a single exponential function, as follows:

$$\mathrm{NEE} = K_0 \,.\, exp\,(K_1 \,.\, Ta) \tag{10.2}$$

where k_0 and k_1 are coefficients, and Ta is air temperature. As a result of fitting Eq. (10.2) to whole available nighttime data, the most important index of temperature sensitivity of respiration $Q_{10} = \exp(k_1)$ was 2.1, and nighttime NEE at air temperature of 10°C was 1.1 μmol m^{-2} s^{-1}.

Time-series of the daily-integrated NEP (= −NEE), precipitation (Pr), global photosynthetic active radiation (PAR), daily maximum of vapor pressure deficit

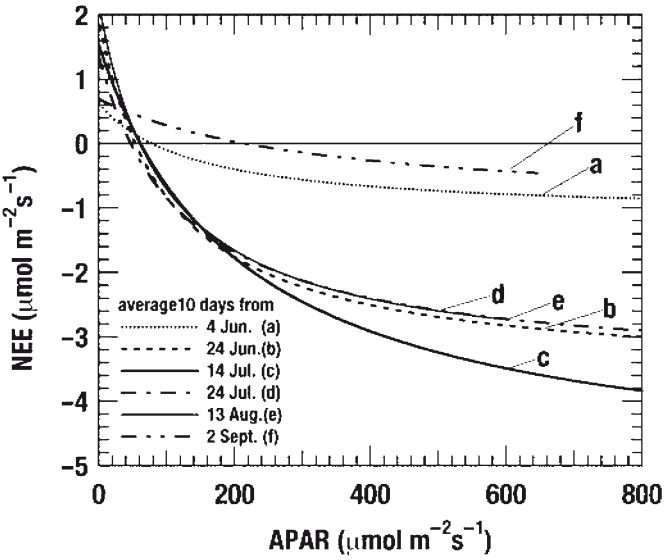

Fig. 10.10 Relationships between daytime net ecosystem exchange of CO_2 (NEE) and absorbed photosynthetic active radiation (APAR) for 10-day periods: (a) 4–13 June; (b) 24 June–3 July; (c) 14–23 July; (d) 24 July–2 August; (e) 13–22 August; and (f) 2–11 September. Each curve was fitted by Eq. (10.1)

(VPDmax), and daily average of air temperature and soil temperature are shown in Fig. 10.7. The cumulative NEP for the whole measurement period of 91 days was 76–78 gC m^{-2}. Daily NEP was near zero in early June, sharply increased by the end of June, and reached a seasonal maximum of 2.0 gC $m^{-2}d^{-1}$ between late June and mid-July. Thereafter, it decreased by late August, and became negative in early September. This seasonal variation indicates that net uptake by the ecosystem continued from early June to mid-August, reaching a maximum between late June and mid-July, and the ecosystem began to release CO_2 after late August.

Seasonal change in NEP during the early growing season could be primarily related to needle phenology of the larch trees. Namely, during a few-week-period of needle growth after bud-break in early and mid-June, daily net uptake sharply increased to the seasonal maximum (Fig. 10.7c), though no visible signs of seasonal growth were observed for the most species of ground vegetation (i.e., woody shrubs). This coincidence between the patterns of NEP and plant phenology suggests that net CO_2 uptake in the early growing season largely depends on photosynthetic activity of the larch trees. On the other hand, daily net CO_2 uptake decreased gradually from late July to the end of August. In this period, canopy photosynthetic activity may still have continued at least until late August, because senescence of larch needles occurred in early September or later. However, both air temperature and incident radiation have already begun to decline in late July (Fig. 10.7b, d), suggesting that NEE of the larch ecosystem might be mostly governed by seasonal changes in air temperature and incoming radiation rather than photosynthetic activities of larch needles during latter half of the growing season (late July to August).

The bud-break and flushing of *L. gmelinii* needles may be triggered by soil surface thawing in the spring (Kujansuu et al. 2007; also see Chap. 17, this Vol.). Air temperature and soil temperature data from 2004 to 2005 at Tura Hydro-meteorological Station (Fig. 10.6) show that thawing of the soil surface continued for several days (indicated as "melting period" in Fig. 10.6 when soil temperature remains near zero) and was completed in early May 2005, after which bud break occurred in mid-May near the station. Consequently, close relationships between the energy budgets over the soil surface and phenological characteristics could be a key issue in the CO_2 budget of larch ecosystems.

Daily maximum of half-hourly or hourly CO_2 uptake rates during midsummer reached 3–6 μmol $m^{-2} s^{-1}$. Table 10.3 lists the maximum values of half-hourly or hourly NEP (=−NEE) mainly for old larch forests and other boreal forests. The NEP value of *L. gmelinii* forest at Tura is considerably lower than that of other boreal forests. This may be primarily due to smaller leaf area index (LAI = ca. 0.6 ha ha^{-1}) of a typical old stand on permafrost compared to that of other forests (LAI = 1–4 ha ha^{-1}). Thus, cumulative NEP (70–80 gC m^{-2} for 91 days) during a growing season was also much lower than that (290 gC m^{-2} for 100 days) of the larch forest near Yakutsk with LAI of ca. 3.7 ha ha^{-1} (Dolman et al. 2004).

Lower cumulative value of CO_2 uptake could be associated not only with low LAI, but also with other environmental factors, such as short growing periods, typically beginning in late May or early June and ending in early September (i.e., only three months or less). Moreover, low soil temperature and shallow depth of soil active layer may make productivity of the larch forest lower. In fact, the maximum depth of soil active layer is shallower (ca. 0.7 m) in the present study site (Kajimoto et al. 2007) than in the larch forest near Yakutsk (1.2 m) (Dolman et al. 2004). In winter, NEE may be slightly positive due to gradual release of CO_2 from accumulated snow or frozen soils to the atmosphere as suggested in many forest ecosystems. Sum of such CO_2 release in winter is probably negligibly small in the stand of the present study (T. Morishita et al. personal communication). For further discussion of seasonal and annual NEE of typical old larch forests in the region, multi-year measurements are needed to ascertain how representative is the seasonal NEE during a single growing season. For evaluation of annual NEE, it is also necessary to estimate CO_2 exchange during winter by applying technically more difficult chamber measurements and continuous meteorological observations.

Additionally, water balance in the region of continuous permafrost is also globally an important theme (see Chap. 13, this Vol.). According to preliminary analysis, cumulative precipitation and evapotranspiration (probably without interception evaporation) were mostly comparable at the present study site during the measurement period. Daily evapotranspiration averaged 1.3 mm d^{-1} and reached the maximum of 2.4 mm d^{-1} (Y. Nakai, unpubl. data). Further analysis of water vapor fluxes, especially gap-filling, would still be needed for discussion of long-term evapotranspiration.

Table 10.3 Maximum NEP (half-hourly or hourly) at midday of midsummer, annual precipitation, and stand characteristics of boreal forests

Forest type	Location	Site ID (name)	Annual precipitation (mm)	Maximum NEP ($\mu mol\ m^{-2}\ s^{-1}$)	LAI	Stand height (m)	Mean DBH (cm)	Stand age (year)	Reference
Aspen	53.629°N, 106.200°W, 601 m a.s.l.	Boreal ecosystem–atmosphere study (BOREAS) SSA-OA	406	10–20	2.1	20	20.5	84	Black et al. (1996)
Black spruce	55.879°N, 98.484°W, 259 m a.s.l.	BOREAS NSA-OBS	517	4–10	2.3	9.1	8.5	155	Goulden et al. (1997)
Black spruce	53.987°N, 105.118°W, 629 m a.s.l.	BOREAS SSA-OBS	405	6–9	2.6	11	8	115	Jarvis et al. (1997)
Jack pine	53.916°N, 104.692°W, 579 m a.s.l.	BOREAS SSA-OJP,	405	8–12	1.4	13	17	65	Baldocchi et al. (1997)
Scot pine	61.850°N, 24.283°E, 181 m a.s.l.	Hyytiälä, Finland	709	10–16	4	14	–	40 plantation	Markkanen et al. (2001)
Scot pine	60.75°N, 89.23°E, 90 m a.s.l.	Zotino, Central Siberia	565	8–12	1.5	–	–	200	Lloyd et al. (2002)
birch	60.968°N, 89.717°E, 200 m a.s.l.	Zotino, Central Siberia	597	10–20	–	18	12	50	Meroni et al. (2002)
Mountain birch	69.467°N, 27.233°E, 280 m a.s.l.	Petsiko, northern Finland	–	4–7	2.5	3.5	–	–	Aurela et al. (2001)
Larch	48.4°N, 108.7°E, 1,630 m a.s.l.	Mongolia	282	7–10	2.2	20	15	>150	Li et al. (2005)

(continued)

Table 10.3 (continued)

Forest type	Location	Site ID (name)	Annual precipitation (mm)	Maximum NEP ($\mu mol\ m^{-2}\ s^{-1}$)	LAI	Stand height (m)	Mean DBH (cm)	Stand age (year)	Reference
Larch	42.7°N, 141.5°E, 125 m a.s.l.	Tomakomai, Hokkaido Japan	1,132	15–25	2.1	14	18	45	Wang et al. (2004)
Larch	45.3°N, 127.6°E, 340 m a.s.l.	Laoshan, China	724	20–35	2.5	18	–	–	Wang et al. (2005)
Larch (CP[a])	60.9°N, 128.3°E, 348 m a.s.l.	SW of Yakutsk	213	3–7	1.4	16	–	125	Hollinger et al. (1998)
Larch (CP[a])	62.3°N, 129.2°E, 220 m a.s.l.	Spasskaya Pad, Yakutsk	240	7–15	3.7	18	–	160	Dolman et al. (2004)
Larch (CP[a])	64.2°N, 100.5°E, 250 m a.s.l.	Tura, Central Siberia	360	3–5	0.6	3.5	3.1	105	Nakai et al. (2008)
High arctic fen, (CP[a])	74.5°N, 20.6°W, <200 m a.s.l.	Zackenberg, Greenland	214	2–4	1.1	0.13	–	–	Nordstroem et al. (2001)

[a]"CP" denotes continuous permafrost region

10.5 Conclusions

NEE of CO_2 in permafrost *Larix gmelinii* forests in Central Siberia can be summarized as follows.

- Information on carbon budget of larch forests is still limited compared to boreal forests in other regions. However, stable operation of tower flux measurements at remote sites is possible during growing seasons using the eddy covariance technique and solar power.
- Typical rates of CO_2 uptake and release by this 105-year-old are as follows: Maximum of half-hourly net CO_2 uptake rates during midsummer ranged from 3 to 5 μmol $m^{-2} s^{-1}$; Maximum of daily net uptake of CO_2 during the growing season was about 2 gC $m^{-2} d^{-1}$, occurring between late June and mid-July.
- In comparison to other boreal forests, magnitude of net CO_2 uptake and cumulative net CO_2 uptake were low. Lower net CO_2 uptake of this permafrost larch forest may be primarily associated with its small leaf area index, and is further influenced by the environmental factors characteristics to the permafrost region (e.g., low soil temperature, short growing season). Initiation and following increase in CO_2 uptake were closely related to phenological development of larch needles.

Directions that should be needed for further understanding of NEE of CO_2 in typical open-canopy old larch forests in the permafrost region of Siberia would be:

- To continue longer-term and multiyear measurements. This could clarify functions of permafrost larch forests.
- To partition entire ecosystem exchange into contributions of ground vegetation and of larch trees.
- To clarify and model phenology of larch trees in the permafrost Siberia.

Acknowledgments I appreciate the assistance of Y. Matsuura, T. Kajimoto, and A. Osawa for discussions and manuscript preparation. I am grateful to late A.P. Abaimov, O.A. Zyryanova, and colleagues of V.N. Sukachev Institute of Forest for their help in various aspects of the field work. Thanks are due to V.M. Borovikov and colleagues of Evenkia Department of Forestry in Tura for their support in logistics and instrumentation. I also thank T. Yorisaki, H. Tanaka, and staff of Climatec Inc. for system integration and instrumentation. I acknowledge Y. Ohtani, T. Watanabe, and Y. Yasuda for providing software resources. S. Yamamoto and N. Saigusa encouraged me greatly. This research was funded by the "Global environment research fund S-1," as "Integrated Study for Terrestrial Carbon Management of Asia in the twentyfirst Century based on Scientific Advancements (FY2002–2006)."

References

Abaimov AP, Lesinski JA, Martinsson O, Milyutin LI (1998) Variability and ecology of Siberian larch species. Swedish University of Agricultural Sciences, Department of Silviculture Reports 43, Umeå, p 118

Abaimov AP, Erkalov AV, Prokushkin SG, Matsuura Y, Osawa A, Kajimoto T, Takenaka A (2000) The conservation and quality of Gmelin larch seeds in cryolithic zone of Central Siberia. In: Inoue G, Takenaka A (eds) Proceedings of the Eighth Symposium on the Joint Siberian Permafrost Studies between Japan and Russia in 1999. National Institute for Environmental Studies, Tsukuba, pp 3–9

Aurela M, Tuovinen JP, Laurila T (2001) Net CO_2 exchange of a subarctic mountain birch ecosystem. Theor Appl Climatol 70:135–148

Baldocchi DD, Vogel CA, Hall B (1997) Seasonal variation of carbon dioxide exchange rates above and below a boreal jack pine forest. Agr For Meteorol 83:147–170

Black TA, den Hartog G, Neumann HH, Blanken PD, Yang PC, Russell C, Nesic Z, Lee X, Chen SG, Staebler R, Novak MD (1996) Annual cycles of water vapour and carbon dioxide fluxes in and above a boreal aspen forest. Global Change Biol 2:219–229

Bondarev A (1997) Age distribution patterns in open boreal Dahurican larch forests of Central Siberia. Forest Ecol Manage 93:205–214

Dolman AJ, Maximov TC, Moors EJ, Maximov AP, Elbers JA, Kononov AV, Waterloo MJ, van der Molen MK (2004) Net ecosystem exchange of carbon dioxide and water of far eastern Siberian Larch (*Larix cajanderii*) on permafrost. Biogeosciences 1:133–146

Foken Th, Wichura B (1996) Tools for quality asessment of surface-based flux measurements. Agr For Meteorol 78:83–105

Goulden ML, Daube BC, Fan S-M, Sutton DJ, Bazzaz A, Munger JW, Wofsy SC (1997) Physiological responses of a black spruce forest to weather. J Geophys Res 120:28987–28996

Grelle A, Burba G (2007) Fine-wire thermometer to correct CO_2 fluxes by open-path analyzers for artificial density fluctuations. Agric For Meteorol 147:48–57

Halldin S, Gryninig S-E, Gottschalk L, Jochum A, Lundin L-C, Van de Griend AA (1999) Energy, water and carbon exchange in a boreal forest landscape — NOPEX experiences. Agr Forest Meteorol 98–99:5–29

Hirano T, Hirata R, Fujinuma Y, Saigusa N, Yamamoto S, Harazono Y, Takada M, Inukai K, Inoue G (2003) CO_2 and water vapor exchange of a larch forest in northern Japan. Tellus 55B:244–257

Hollinger DY, Kelliher FM, Byers JN, Hunt JE, McSeveny TM, Weir PL (1994) Carbon dioxide exchange between an undisturbed old-growth temperate forest and the atmosphere. Ecology 75:134–150

Hollinger DY, Kelliher FM, Schulze E-D, Vygodskaya NN, Varlargin A, Milukova I, Byers JN, Sogatchev A, Hunt JE, McSeveny TM, Kobak KI, Bauer G, Arneth A (1995) Initial assessment of multi-scale measurements of CO_2 and H_2O flux in the Siberian taiga. J Biogeogr 22:425–431

Hollinger DY, Kelliher FM, Schulze ED, Bauer G, Arneth A, Byers JN, Hunt JE, McSeveny TM, Kobak KI, Milukova I, Sogatchev A, Tatarinov F, Varlargin A, Ziegler W, Vygodskaya NN (1998) Forest-atmosphere carbon dioxide exchange in eastern Siberia. Agr For Meteorol 90:291–306

Jarvis PG, Massheder JM, Hale SE, Moncrieff JB, Rayment M, Scott SL (1997) Seasonal variation of carbon dioxide, water vapor, and energy exchanges of a boreal black spruce forest. J Geophys Res 120:28953–28966

Jarvis PG, Saugier B, Schulze E-D (2001) Productivity of boreal forests. In: Roy J, Saugier B, Mooney HA (eds) Terrestrial global productivity. Academic Press, New York, pp 211–244

Kajimoto T, Matsuura Y, Sofronov MA, Volokitina AV, Mori S, Osawa A, Abaimov AP (1999) Above- and belowground biomass and net primary productivity of a *Larix gmelinii* stand near Tura, central Siberia. Tree Physiol 19:815–822

Kajimoto T, Matsuura Y, Osawa A, Prokushkin AS, Sofronov MA, Abaimov AP (2003) Root system development of *Larix gmelinii* trees affected by micro-scale conditions of permafrost soils in central Siberia. Plant Soil 255:281–292

Kajimoto T, Matsuura Y, Osawa A, Abaimov AP, Zyryanova OA, Ishii A, Kondo K, Tokuchi N (2004) Biomass and spatial patterns of individual root system in *Larix gmelinii* stands on

continuous permafrost region of central Siberia. In: Tanaka H (ed) Proceeding of the Fifth International Conference on Global Change: Connection to the Arctic (GCCA-5). Tsukuba University, Tsukuba, pp 187–190

Kajimoto T, Matsuura Y, Osawa A, Abaimov AP, Zyryanova OA, Isaev AP, Yefremov DP, Mori S, Koike T (2006) Size-mass allometry and biomass allocation of two larch species growing on the continuous permafrost region in Siberia. For Ecol Manage 222:314–325

Kajimoto T, Osawa A, Matsuura Y, Abaimov AP, Zyryanova OA, Kondo K, Tokuchi N, Hirobe M (2007) Individual-based measurement and analysis of root system development: case studies for *Larix gmelinii* trees growing on the permafrost region in Siberia. J For Res 12:103–112

Kelliher FM, Hollinger DY, Schulze E-D, Vygodskaya NN, Byers JN, Hunt JE, McSeveny TM, Milukova I, Sogatchev A, Varlargin A, Ziegler W, Arneth A, Bauer G (1997) Evaporation from an eastern Siberian larch forest. Agr For Meteorol 85:135–147

Kujansuu J, Yasue K, Koike T, Abaimov AP, Kajimoto T, Takeda T, Tokumoto M, Matsuura Y (2007) Responses of ring widths and maximum densities of *Larix gmelinii* to climate on contrasting north- and south-facing slopes in central Siberia. Ecol Res 22:582–592

Li S-G, Asanuma J, Kotani A, Eugster W, Davaa G, Oyunbaatar D, Sugita M (2005) Year-round measurements of net ecosystem CO_2 flux over a montane larch forest in Mongolia. J Geophys Res . doi:10.1029/2004JD005453

Lloyd J, Shibistova OB, Zolotoukhine D, Kolle O, Arneth A, Wirth C, Styles JM, Tchebakova NM, Schulze E-D (2002) Seasonal and annual variations in the photosynthetic productivity and carbon balance of a central Siberian pine forest. Tellus 54B:590–610

Lydolph PE (1977) Climates of the Soviet Union. World survey of climatology, vol 7. Elsevier, Amsterdam, p 417

Machimura T, Kobayashi Y, Iwahana G, Hirano T, Lopez L, Fukuda M (2005) Change of carbon dioxide budget during three years after deforestation in eastern Siberian larch forest. J Agric Meteorol 60:653–656

Markkanen T, Rannik Ü, Keronen P, Suni T, Vesala T (2001) Eddy covariance fluxes over a boreal Scots pine forest. Boreal Environ Res 6:65–78

Matsuura Y, Abaimov AP (2000) Nitrogen mineralization in larch forest soils of continuous permafrost region, Central Siberia: An implication for nitrogen economy of a larch forest stand. In: Inoue G, Takenaka A (eds) Proceedings of the Eighth Symposium on the Joint Siberian Permafrost Studies between Japan and Russia in 1999. National Institute for Environmental Studies, Tsukuba, pp 129–134

Matsuura Y, Kajimoto T, Osawa A, Abaimov AP (2005) Carbon storage in larch ecosystems in continuous permafrost region of Siberia. Phyton 45:51–54

McMillen RT (1988) An eddy correlation technique with extended applicability to non-simple terrain. Boundary-Layer Meteorol 43:231–245

Meroni M, Mollicone D, Belelli L, Manca G, Rosellini S, Stivanello S, Tirone G, Zompanti R, Tchebakova N, Schulze ED, Valentini R (2002) Carbon and water exchanges of regenerating forests in central Siberia. For Ecol Manage 169:115–122

Nakai Y, Matsuura Y, Kajimoto T, Abaimov AP, Yamamoto S (2004) CO_2 flux measurements above a larch forest in a continuous permafrost region of Central Siberia using eddy covariance techniques (preliminary results). In: Tanaka H (ed) Proceeding of the Fifth International Conference on Global Change Connection to the Arctic (GCCA5). Tsukuba University, Tsukuba, pp 160–163

Nakai Y, Matsuura Y, Kajimoto T, Abaimov AP, Yamamoto S (2005) Eddy covariance CO_2 flux above a Gmelin larch forest on continuous permafrost of Central Siberia during two Growing Seasons. In: Proceedings of the Sixth International Conference on Global Change Connection to the Arctic (GCCA6), Tokyo, pp 169–172

Nakai T, van der Molen MK, Gash JHC, Kodama Y (2006) Correction of sonic anemometer angle of attack errors. Agr For Meteorol 136:19–30

Nakai Y, Matsuura Y, Kajimoto T, Zyryanova OA, Yamamoto S (2007) Water and CO_2 exchange at a Gmelin larch forest on continuous permafrost of Central Siberia during growing Seasons.

Proceedings of the Seventh International Conference on Global Change Connection to the Arctic (GCCA7). International Arctic Research Center, University of Alaska, Fairbanks, pp 263–266

Nakai Y, Matsuura Y, Kajimoto T, Abaimov AP, Yamamoto S, Zyryanova OA (2008) Eddy covariance CO_2 flux above a Gmelin larch forest on continuous permafrost of Central Siberia during a growing season. Theor Appl Climatol 93:133–147

Nordstroem C, Soegaard H, Christensen TR, Friborg T, Hansen BU (2001) Seasonal carbon dioxide balance and respiration of a high-arctic fen ecosystem in NE-Greenland. Theor Appl Climatol 70:149–166

Ohta T (2005) Spatial variation of the parameters of canopy conductance model in temperate and boreal forests. Proceedings of the International Semi-Open Workshop on C/H_2O/Energy Balance and Climate over Boreal Regions with Special Emphasis on Eastern Eurasia. Yakutsk, Russia, pp 87–90

Ohta T, Hiyama T, Tanaka H, Kuwada T, Maximov TC, Ohata T, Fukushima Y (2001) Seasonal variation in the energy and water exchanges above and below a larch forest in eastern Siberia. Hydrol Proc 15:1459–1476

Ohta T, Maximov TC, Dolman AJ, Nakai T, van der Molen MK, Kononov AV, Maximov AP, Hiyama T, Iijima Y, Moors EJ, Tanaka H, Toba T, Yabuki H (2008) Interannual variation of water balance and summer evapotranspiration in an eastern Siberian larch forest over a 7-year period (1998–2006). Agr For Meteorol . doi:10.1016/j.agrformet.2008.04.012

Ohtani Y, Mizoguchi Y, Watanabe T, Yasuda Y (2005) Parameterization of NEP for gap filling in a cool-temperate coniferous forest in Fujiyoshida, Japan. J Agric Meteorol 60:769–772

Osawa A, Abaimov AP, Zyryanova OA (2000) Tree size-density relationship and size-dependent mortality in *Larix gmelinii stands*. In: Inoue G, Takenaka A (eds) Proceedings of the Eighth Symposium on the Joint Siberian Permafrost Studies between Japan and Russia in 1999, Tsukuba, pp 36–41, 2000

Osawa A, Abaimov AP, Matsuura Y, Kajimoto T, Zyryanova OA (2003) Anomalous patterns of stand development in larch forest of Siberia. Tohoku Geophysic J (Sci Rep Tohoku Univ Ser 5) 36:471–474

Osawa A, Abaimov AP, Kajimoto T, Matsuura Y, Zyryanova OA, Tokuchi N, Kondo K, Hirobe M (2004) Long-term development of larch forest ecosystems on continuous permafrost of Siberia: structural constraints and implications to carbon accumulation. In: Tanaka H (ed) Proceeding of the Fifth International Conference on Global Change: Connection to the Arctic (GCCA-5). Tsukuba University, Tsukuba, pp 53–56

Röser C, Montagnani L, Schulze E-D, Mollicone D, Kolle O, Meroni M, Papale D, Marchesini LB, Federici S, Valentini R (2002) Net CO_2 exchange rates in three different successional stages of the "Dark Taiga" of central Siberia. Tellus 54B:642–654

Ruimy A, Jarvis PG, Baldocchi DD, Saugier B (1995) CO_2 fluxes over plant canopies and solar radiation: a review. Adv Ecol Res 26:1–98

Schulze E-D, Lloyd J, Kelliher FM, Wirth C, Rebmann C, Luhker B, Mund M, Knohl A, Milyukova I, Schulze W, Ziegler W, Varlagin A, Sogachov A, Valentini R, Dore S, Grigoriev S, Kolle O, Tchebakova N, Vygodskaya NN (1999) Productivity of forests in the Eurosiberian boreal region and their potential to act as a carbon sink - a synthesis. Global Change Biol 5:703–722

Sellers PJ, Hall FG, Kelly RD, Black A, Baldocchi D, Berry J, Ryan M, Ranson KJ, Crill PM, Lettenmaier DP, Margolis H, Cihlar J, Newcomer J, Fitzjarrald D, Jarvis PG, Gower ST, Halliwell D, Williams D, Goodison B, Wickland DE, Guertin FE (1997) BOREAS in 1997: Experiment overview, scientific results, and future directions. J Geophys Res 120:28731–28769

Shibistova O, Lloyd J, Zrazhevskaya G, Arneth A, Kolle O, Knohl A, Astrakhantceva N, Shijneva I, Schmerler J (2002) Annual ecosystem respiration budget for a *Pinus sylvestris* stand in central Siberia. Tellus 54B:568–589

Tokuchi N, Kondo K, Hirobe M, Matsuura Y, Kajimoto T (2004) N cycling at Larix stand in Tura, Central Siberia –Spatial variability of soil N dynamics- In: Tanaka H (ed) Proceeding of the Fifth International Conference on Global Change: Connection to the Arctic (GCCA-5). Tsukuba University, Tsukuba, pp 207–209

Vickers D, Mahrt L (1997) Quality control and flux sampling problems for tower and aircraft data. J Atmos Ocean Tech 14:512–526

Wang H, Saigusa N, Yamamoto S, Kondo H, Hirano T, Toriyama A, Fujinuma Y (2004) Net ecosystem CO_2 exchange over a larch forest in Hokkaido, Japan. Atmos Environ 38:7021–7032

Wang H, Zu Y, Saigusa N, Yamamoto S, Kondo H, Yang F, Wang W (2005) CO2, water vapor and energy fluxes in a larch forest in northeast China. J Agric Meteorol 60:549–552

Webb EK, Pearman GI, Leuning R (1980) Correction of flux measurements for density effects due to heat and water vapor transfer. Q J Roy Meteorol Soc 106:85–100

Wilson K, Goldstein A, Falge E, Aubinet M, Baldocchi D, Berbigier P, Bernhofer C, Ceulemans R, Dolman H, Field C, Grelle A, Ibrom A, Law BE, Kowalski A, Meyers T, Moncrieff J, Monson R, Oechel W, Tenhunen J, Valentini R, Verma S (2002) Energy balance closure at FLUXNET sites. Agr For Meteorol 113:223–243

Zyryanova OA, Shitova SA (1999) Spatial distribution regularities of the central Evenkain larch forests: a cartographic model. In: Fukuda M (ed) Proceedings of the Fourth Symposium on the Joint Siberian Permafrost Studies between Japan and Russian in 1995. Hokkaido University, Sapporo, pp 65–69

Zyryanova OA, Abaimov AP, Bugaenko TN, Bugaenko NN (2000) Larch plant associations diversity of Central Siberian cryolithic zone and the development of the database. In: Inoue G, Takenaka A (eds) Proceedings of the eighth Symposium on the Joint Siberian Permafrost Studies between Japan and Russia in 1999. National Institute for Environmental Studies, Tsukuba, pp 83–89